P AND S WAVE VELOCITY STRUCTURE OF THE CRUST AND UPPER MANTLE UNDER CHINA AND SURROUNDING AREAS FROM BODY AND SURFACE WAVE TOMOGRAPHY

M. Nafi Toksöz, Robert D. Van der Hilst, Youshun Sun, Chang Li, and Huajian Yao

Massachusetts Institute of Technology

Sponsored by Air Force Research Laboratory

Contract No. FA8718-04-C-0018

ABSTRACT

The objective of this project is to use a combination of travel-time and surface wave tomography to obtain compressional and shear wave velocity distributions in the crust and upper mantle under China and surrounding areas.

Three-dimensional (3-D) P and S wave velocity structures, based on travel-time tomography, are developed for the crust and the upper mantle transition zone for China and surrounding areas. P and S wave arrival time data from the Annual Bulletin of Chinese Earthquakes (ABCE) are used for the regional travel-time tomography of the crust and uppermost mantle. The International Seismology Centre (ISC/EHB) travel times are used with the crustal structure to extend the velocity models into the mantle. The shallow velocity models correlate well with the major geologic features, such as the Tibet Plateau and the basins. P and S wave velocity structures in general are well-correlated. Lateral variations of shear velocities, which exceed 6% at some places, are larger than P velocity variations.

The current effort is directed to two areas: (1) obtaining a regional crust/uppermost mantle 3-D shear wave velocity model from the travel times and (2) obtaining high-resolution, regional velocity models where additional data from local networks make it feasible to undertake the tomographic inversions. Tibet and southwestern regions are the primary regions in these studies.

OBJECTIVES

The primary goal of this project is to obtain compressional and shear wave velocity distributions in the crust and upper mantle under China and surrounding areas using a combination of travel-time and surface wave tomography. The first phase of the study is directed at producing a P wave velocity model based on travel-time tomography.

RESEARCH ACCOMPLISHED

Introduction

In this paper we present a 3-D shear wave velocity structure for the crust and upper mantle under China and surrounding regions obtained using local and regional travel-times and surface waves.

The available S wave velocity models of the crust and upper mantle in China and the surrounding area have been obtained using different approaches. Global models such as CUB 1.0 (Shapiro and Ritzwoller, 2002) and the SAIC 1° x 1° model (Stevens et al., 2001) were constructed from group and phase velocity dispersion measurements of surface waves. The global model CRUST 2.0 (Laske et al., 2001) was constructed from seismic refraction data and developed from the CRUST 5.1 model (Mooney, 1998) and a 1° x 1° sediment map (Laske and Masters, 1997). Only P wave velocities are inverted by travel-time tomography. The S wave velocities in the model are obtained by empirical Vp/Vs ratios or compiled from other sources. For East Asia, mantle S velocity models were obtained from shear and surface waveforms (Friederich, 2003). Lateral spatial resolution of the models is larger than 200 km.

Regional models were constructed by Sn and/or Pn tomography (Ritzwoller et al., 2002; Hearn and Ni, 2001; Pei et al., 2004) and from surface waves (Wu et al., 1997, Lebedev and Nolet, 2003; Huang et al., 2002; Song et al. 1991; Zhu et al., 2002). P and S wave tomography have been performed in several local regions in China (Xu et al., 2002; Huang et al., 2002; Yu et al., 2003; Huang and Zhao, 2004;). Xu et al. (2002) used P and S wave arrival times of local, regional and teleseismic events recorded by Chinese and Kyrgyzstan seismic networks to derive crust and upper mantle velocity structures beneath western China. The grid spacing is 1.5° x 1.5° in the horizontal direction and about 10 km (in the crust) and 50 km (in uppermost mantle) in the vertical direction. Crustal structure models beneath north and east China, including Beijing and surrounding regions, were obtained by Zhu et al. (1990), Yu et al. (2003) and Huang and Zhao (2004) with a P and S wave tomography. Huang et al. (2002) inverted the lithospheric structure in southwest China from local/regional travel-time data. A number of studies carried out in the Tien Shan (Roecker et al., 1993; Poupinet et al., 2002; Vinnik et al., 2002, 2004) and Hindukush (Koulakov and Sobolev, 2006) regions, that include parts of western China, show heterogeneous crust/upper mantle structures with crustal thickness varying between 40 and 70 km. All these models provide detailed crustal structures in specific regions. A detailed map for the whole China area remains to be developed.

During the last two decades, many digital seismic stations were installed in China. The large database of high-quality recorded arrival times provides an unprecedented opportunity to determine a detailed 3-D crustal structure under the region. Using these data, Sun and Toksöz (2006) derived a 3-D P wave velocity structure for the crust and uppermost mantle. In the present work, we use the tomographic constraint from the P wave study along with the S wave travel times to determine a 3-D shear wave velocity structure of the crust and upper mantle under this region.

Data and Method

For this work, we selected shear wave arrival time data from the Annual Bulletin of Chinese Earthquakes (ABCE) (IG-CSB, 1990–2002). In this database there are 25,000 earthquakes, 220 stations, and 450,000 S wave ray paths in China and the surrounding areas in the January 1990 to December 2002 time period. Figure 1 shows earthquake epicenters and stations in China. The selection of earthquakes is based on the following criteria: (1) events that occurred in the study area with magnitudes greater than M 3.0 (except for the northwest area with less seismicity, where we included earthquakes with M 2.5–3.0); (2) all selected events were recorded by at least 15 stations; and (3) earthquakes were selected to provide a uniform distribution of hypocenters in the study area. With these criteria, 262,000 S wave arrival times from 12,215 earthquakes were selected to determine the S wave velocity structure. The reading accuracy of S wave arrival times is, in general, 0.1–0.4 s. Figure 1 shows the epicentral distribution of the 12,215 selected earthquakes.

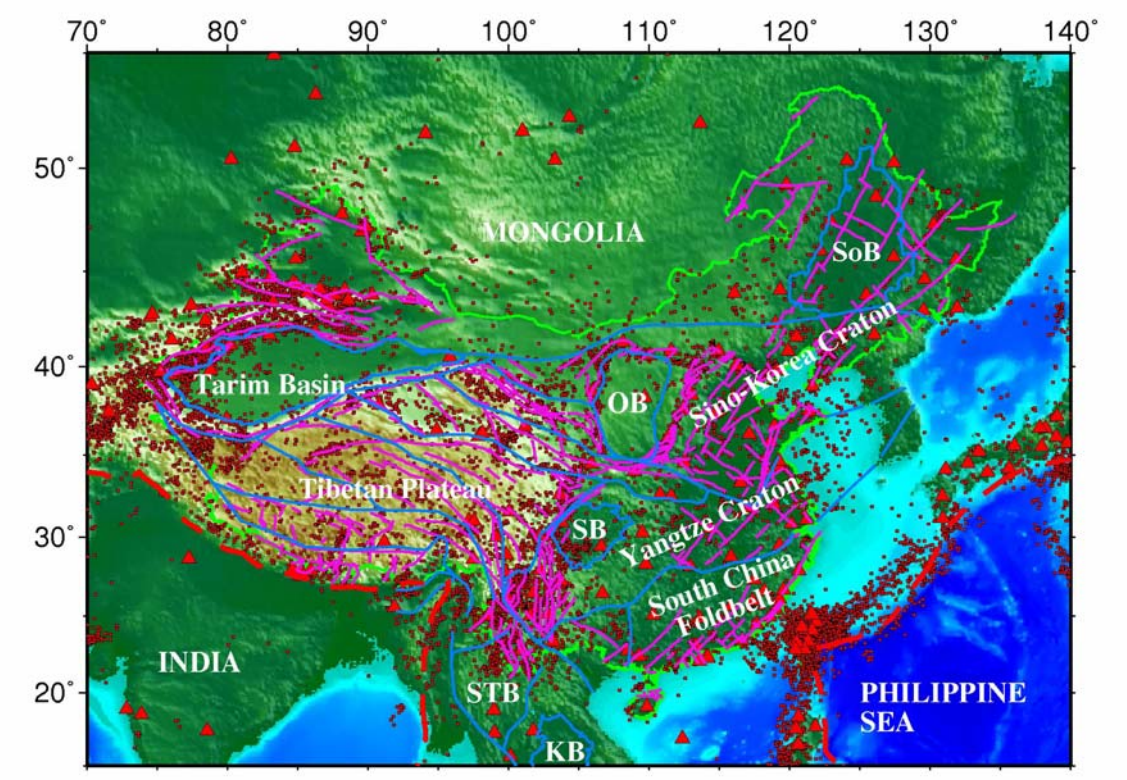

Figure 1. Shown are 512 earthquakes (M > 6.0 from January 1978 to May 2004), 220 stations, active faults, and major tectonic boundaries in China and the surrounding area. Earthquake epicenters are shown in red dots and stations are shown in red triangles. The yellow line shows the boundary of China. Active faults in the China area are shown in purple lines and tectonic sutures are shown in blue lines, where SoB: Songliao Basin; OB: Ordos Basin; SB: Sichuan Basin; KB: Khorat Basin; STB: Shan Thai Block; IB: Indochina Block.

To determine the shear velocity structure from arrival time data, we used the tomographic method of Zhao et al. (1992). This method has the following features: (1) It accommodates discontinuities such as the Moho. A 3-D grid is set up in the model to express the 3-D structure. Velocity perturbations at the grid nodes are the unknown parameters. The velocity perturbation at any point in the model is calculated by linearly interpolating the velocity perturbation at the eight grid nodes surrounding that point. (2) It calculates travel times and ray paths using an efficient 3-D ray-tracing technique (Zhao et al., 1992). It uses iteratively the pseudobending technique of Um and Thurber (1987). Station elevations are taken into account in the ray tracing. (3) It uses a LSQR algorithm (Paige and Saunders, 1982) with a damping regularization to solve the large and sparse system of equations, inherent in the tomographic problem. The LSQR algorithm has been used by a number of researchers (Nolet, 1985; Spakman and Nolet, 1988; Papazachos and Nolet, 1997), and is an efficient algorithm to solve problems with large sparse systems. (4) The nonlinear tomographic problem is solved by conducting linear inversions iteratively.

For the shear wave tomography we follow a procedure very similar to the one used for the P wave tomography (Sun and Toksöz, 2006). We adopt a grid spacing of 1° × 1° in the horizontal direction, and 10 km in depth. We also set grids at the depths of 1 km, 2 km, 5 km and 7 km to sample the sediment layer. We use a starting 1-D model (Figure 2) based on the average 1-D P wave model. We put into the starting model the Moho depth obtained from the P wave tomography, which is consistent between the Moho depths in this region by different researchers (Mooney, 1998; Hearn et al., 2004; Sun at el, 2004; Sun and Toksöz, 2006). In the study area, the Moho depth ranges from 30 km in the east to 78 km. During the tomographic inversion, the Moho geometry is fixed and only the velocities at grid nodes are determined.

The earthquake hypocentral parameters are those determined by P wave tomography. They are kept constant during S wave inversion. We chose the value of 25.0 for the damping parameters to balance between the reduction of

travel-time residuals and the smoothness of the 3-D velocity model obtained. The root mean square (RMS) travel-time residual decreased by 35% from 0.98 s to 0.72 s by the inversion. Spatial resolution was evaluated using a checkerboard test (Spakman and Nolet, 1988; Zhao et al., 1992).

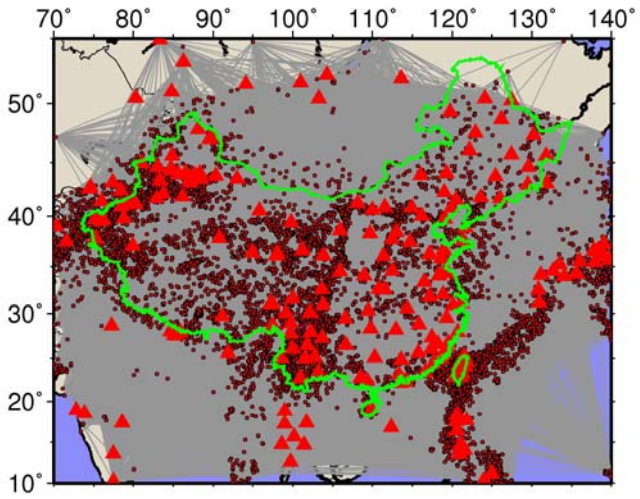

Figure 2. Shown are 25,000 earthquakes, 220 stations, and 450,000 ray paths in China and the surrounding area. Earthquake epicenters are shown in black circles and stations are shown in red triangles. The green line shows the boundary of China.

Results

The 3-D shear wave velocity models are shown in Figures 3–5. Figure 3 shows the Moho depth map taken from P tomography and used as an input to S wave tomography. On the right are the Sn velocities. Depth slices of shear velocities are shown in Figure 4. North-south and east-west cross sections of shear velocities are shown in Figure 5. The lateral variation of S wave velocities exceeds 6% in the study area, indicating the heterogeneities in the crust and upper mantle in this region. Prominent features in the figures are the thick crust under Tibet with low velocity, low Sn velocities in NE China (rift zone) and high Sn velocities under Tibet at 80 km depth.

In the cross sections (Figure 5), there is a prominent low velocity zone in the mid-crust at a depth around 40 km under Tibet. This feature is consistent with other observations of similar velocity decrease and shear wave attenuation increase in the mid- to lower-crust under Tibet. Higher velocities under the Sichuan Basin and under Mount Altay extend into the mantle, as do the lower velocities under the rift system south of the Bohai Bay.

In an earlier study (Sun and Toksöz, 2006), 3-D P wave velocity models were obtained through a tomographic inversion similar to those used in this study for S waves. It would be informative to compare the results. Figure 5 shows N-S cross sections of P and S wave velocities. There is good correlation between the P and S velocities under Tibet. Lower velocities in the mid-crust appear both in the P and S tomograms. The low velocity zone is more prominent in the S velocities.

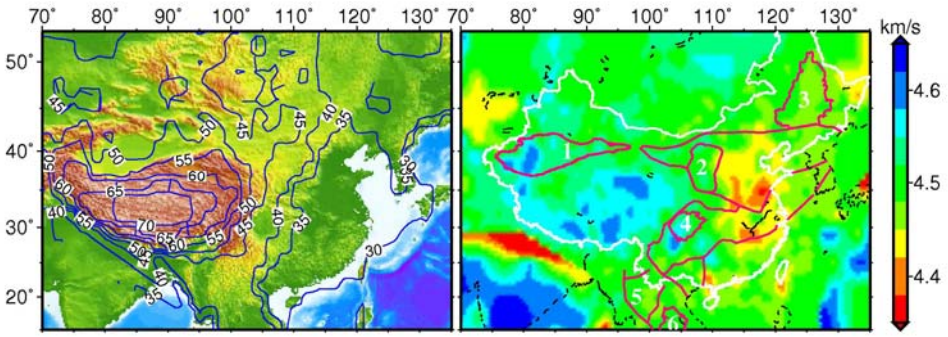

Figure 3. Depth of the Moho discontinuity (left) and Sn velocity distribution obtained (right) in the present study area. The Moho depths are shown in contours. 1: Tarim Basin; 2: Ordos Basin; 3: Songliao Basin; 4: Sichuan Basin; 5: Shan Thai Block; 6: Khorat Basin.

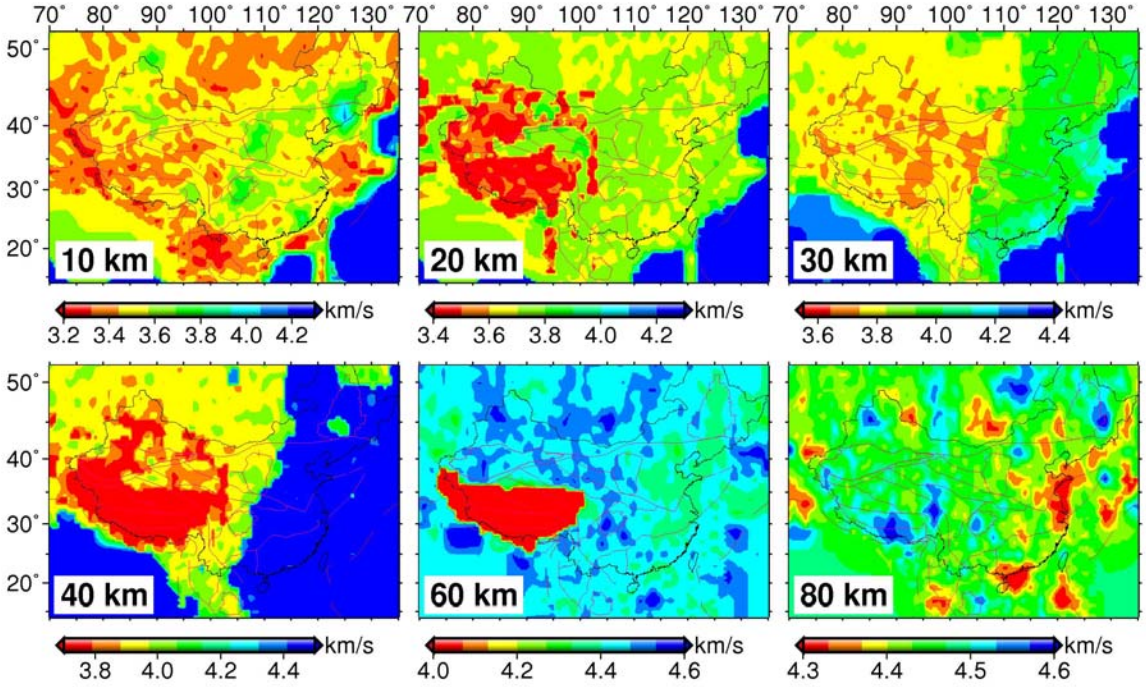

Figure 4. S wave velocity image at each depth slice. The depth of each layer is shown at the lower left corner of each map.

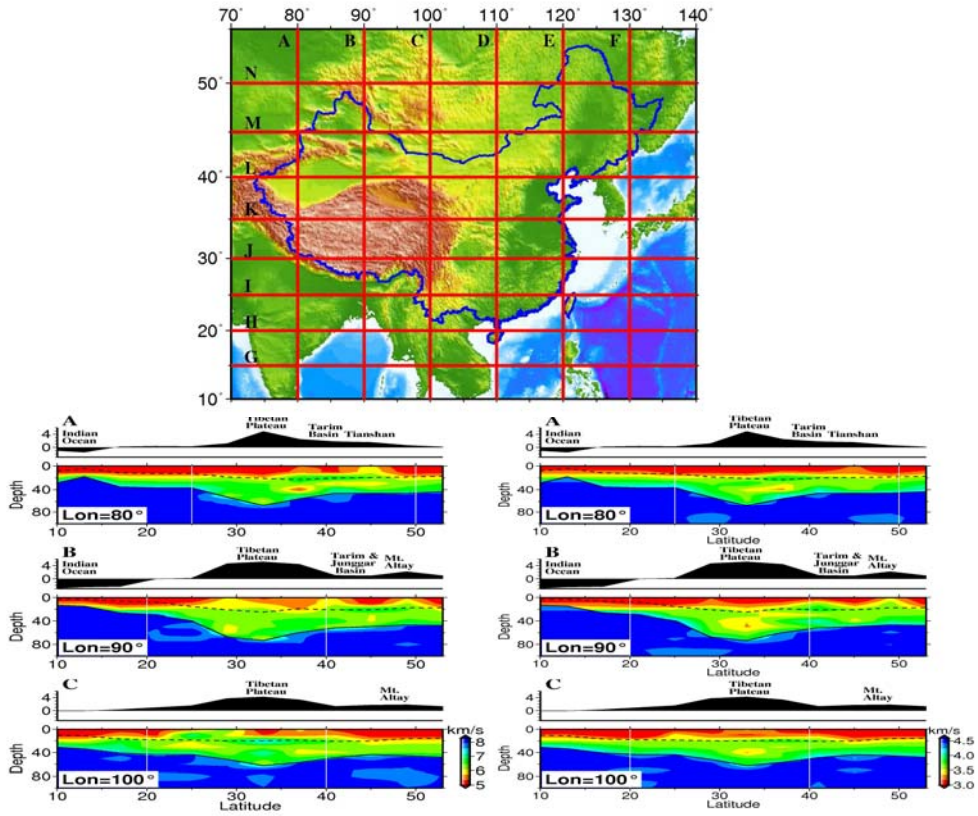

Figure 5. P (left) and S (right) vertical velocity profiles of the crust and uppermost mantle at 80°, 90°, and 100° E longitudes. The profile locations are shown in the upper figure

To extend the velocities into the upper mantle, we use teleseismic travel-time data for P waves and multi-mode surface waves for the shear waves. To minimize the "smearing effect" of crustal structures into the upper mantle, the upper 80 km of the model velocity is constrained by the regional tomography. The regional and teleseismic data from the ISC/EHB database are used for the mantle tomography. The data and tomographic inversion are described by Li et al. (2006). The S wave velocities are obtained by surface wave tomography (Lebedev et al., 2005).

Figure 6 shows the preliminary results for upper mantle P and S wave velocity variations in southern and western China at a depth of 250 km. The color bars and spatial resolutions are different for P and S velocity variations. Note the extension of high velocities under the Sichuan and Ordos basins to 250 km. The relative variations in S wave velocities are greater than those of the P waves.

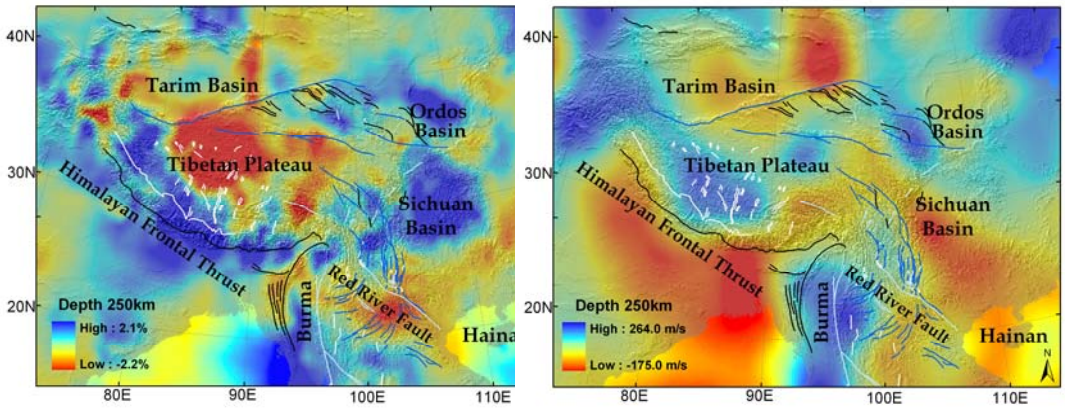

Figure 6. P wave velocity (left) and S wave velocity (right) at the depth of 250 km.

CONCLUSIONS

The 3-D shear-wave velocity models of the crust and upper mantle, obtained by S wave travel-time tomography, reveals pronounced lateral heterogeneities under China and surrounding regions. The velocity models exhibit the following features.

.

1. At the upper crust, down to 20 km depth, velocity variations strongly correlate with the major geological features.

2. There is a strong contrast between the regions to the east of 110°E longitude and the west. In eastern China, where crustal thickness is about 35 km or less, velocity variations are relatively small. Lower velocities delineate the rift structure of NE China. In the region to the west of 110°E longitude the crustal velocities are much more variable. Crustal thickness varies between 35 km and 78 km. The roots of prominent features such as the Tibet, Tarim, Sichuan and Ordos basins, dominate the subsurface velocity structures.

3. There is a prominent low velocity zone in the middle crust (around 40 km depth) under central Tibet. Shear velocity decreases by as much as 6% relative to the values north of Tibet and Tarim basin.

4. In general, there is good correlation between the P wave and S wave velocity variations. However, relative magnitudes of the variations (i.e. percentage velocity changes) are different in different regions. For example, the shear velocity decrease in the mid-crust under Tibet is twice as large as that of P velocity, percentage wise.

5. In the upper mantle, the percentage variation of shear velocities is greater than those of P velocities.

REFERENCES

Friederich, W. (2003). The S velocity structure of the East Asian mantle from inversion of shear and surface waveforms, *Geophys. J. Int.* 153: 88–102.

Hearn, T. M. and J. F. Ni (2001). Tomography and location problems in China using regional travel-time data, in *Proceedings of the 23rd Seismic Research Review: Worldwide Monitoring of Nuclear Explosions*, LA-UR-01-4454, Vol. 1, pp. 27–45.

Hearn, T. M., S. Wang, J. F. Ni, Z. Xu, Y. Yu, and X. Zhang (2004). Uppermost mantle velocities beneath China and surrounding regions, *J. Geophys. Res.* 109: doi:10.1029/2003JB002874.

Huang, J. and D. Zhao (2004). Crustal heterogeneity and seismotectonics of the Chinese capital region. *Tectonophysics* 385: 159–180.

Huang, J., D. Zhao, and S. Zheng (2002). Lithospheric structure and its relationship to seismic and volcanic activity in southwest China. *J. Geophys. Res.* 107: doi:10.1029/2000JB000137.

Institute of Geophysics, China Seismological Bureau (IG-CSB), 1990–2003. *Annual Bulletin of Chinese Earthquakes (ABCE).* Beijing: Seismological Publishing House.

Koulakov, I. and S. V. Sobolev (2006). A tomographic image of Indian lithosphere break-off beneath the Pamir-Hinkukush region, *Geophys. J. Int.* 164: 425–440.

Laske, G. and G. Masters (1997). A global digital map of sediments thickness, *EOS* 78: F483 (abstract).

Laske, G., G. Masters, and C. Reif (2001). CRUST 2.0: A new global crustal model at 2x2 degrees, http://mahi.ucsd.edu/Gabi/rem.dir/crust/crust2.html (last accessed July 2005).

Lebedev, S. and G. Nolet (2003). Upper mantle beneath southeast Asia from S velocity tomography. *J. Geophys. Res.* 108: doi 10.1029/2000JB000073.

Lebedev, S., G. Nolet, T. Meier, and R. D. van der Hilst (2005). Automated multimode inversion of surface and S waveforms, *Geophys. J. Int*. 162: 951–964.

Li, C., R. D. van der Hilst, and M. N. Toksöz (2006). Constraining P wave velocity variations in the upper mantle beneath Southeast Asia, *Phys. Earth Planet. Inter.* 154: 180¨C 195.

Mooney, W. D. (1998). CRUST 5.1: A global crustal model at 5° x 5°. *J. Geophys. Res.* 103: 727–747.

Nolet, G. (1985). Solving and resolving inadequate and noisy tomographic systems, *J. Comput. Phys.* 61: 463–482.

Paige, C. and M. Saunders (1982). LSQR: An algorithm for sparse linear equations and sparse least squares. *ACM Trans. Math. Software* 8: 471.

Papazachos, C. B. and G. Nolet (1997). P and S deep velocity structure of the Hellenic area obtained by robust nonlinear inversion of travel-times, *J. Geophys. Res.* 102: 8,349–8,367.

Pei, S., Z. Xu, and S. Wang (2004). Discussion on origin of Pn velocity variation in China and adjacent region. *Acta Seismol. Sin.* 26: 1–10 (in Chinese).

Poupinet, G., J. P. Avouac, M. Jiang, S. Wei., E. Kissling, G. Herquel, J. Guilbert, A. Paul, G. Wittlinger, H. Su, and J. C. Thomas (2002). Intracontinental subduction and Paleozoic inheritance of the lithosphere suggested by a teleseismic experiment across the Chinese Tien Shan, *Terra Nova* 14: 18–24.

Ritzwoller, M. H., M. P. Barmin, A. Villasenor, A. L. Levshin, and E. R. Engdahl (2002). Pn and Sn tomography across Eurasia to improve regional seismic event locations. *Tectonophys.* 358: 39–55.

Roecker, S. W., T. M. Sabitova, L. P. Vinnik, Y. A. Burmakov, M. I. Golvanov, R. Mamtkanova, and L. Munirova (1993). Three-dimensional elastic wave velocity structure of the western and central Tien Shan, *J. Geophys. Res.* 98: 15,779–15,795.

Shapiro, N. M. and M. H. Ritzwoller (2002). Monte Carlo inversion for a global shear velocity model of the crust and upper mantle. *Geophys. J. Int.* 151: 88–105.

Song, Z. H., C. Q. An, G. Y. Chen, L. H. Chen, Z. Zhuang, Z. W. Fu, and J. F. Hu (1991). Study on 3-D velocity structure and anisotropy beneath west China from the Love wave dispersion. *Acta Geophys. Sin.* 34: 694–707 (in Chinese).

Spakman, W. and G. Nolet (1988). Imaging algorithms, accuracy and resolution in delay time tomography, in *Mathematical Geophysics*, N. Vlar et al. (Eds.). Norwell, Massachusetts: D. Reidel, pp. 155–187

Stevens, J. L., D. A. Adams, and G. E. Baker (2001). Improved surface wave detection and measurement using phase-matched filtering with a global one-degree dispersion model, in *Proceedings of the 23rd Seismic Research Review: Worldwide Monitoring of Nuclear Explosions*, LA-UR-01-4454, Vol. 1, pp 420–430.

Sun, Y. and M.N. Toksöz (2006). Crustal structure of China and surrounding regions from P wave traveltime tomography, *J. Geophys Res.* 111: B03310, doi:10.1029/2005JB003962.

Sun, Y., X. Li, S. Kuleli, F. D. Morgan, and M. N. Toksöz (2004). Adaptive moving window method for 3-D P velocity tomography and its application in China. *Bull. Seism. Soc. Am.* 94: 740–746.

Um, J. and C. Thurber (1987). A fast algorithm for two-point seismic ray tracing. *Bull. Seism. Soc. Am.* 77: 972–986.

Vinnik, L. P., S. W. Roecker, G. L. Kosarev, S. I. Oreshin, and I. Y. Koulakov (2002). Crustal structure and dynamics of the Tien Shan, *Geophys. Res. Lett.* 29: 2047, doi 10.1029/2002GL015531.

Vinnik, L. P. C. Reigber, I. M. Aleshin, G. L. Koserev, M. K. Kaban, S. I. Oreshin, and S. W. Roecker (2004). Receiver function tomography of the central Tien Shan, *Earth Planet. Sci. Lett.* 225: 131–146.

Wu, F. T., A. L. Levshin, and V. M. Kozhevnikov (1997). Rayleigh wave group velocity tomography of Siberia, China, and vicinity. *Pure Appl. Geophys.* 149*:* 447–473.

Xu, Y., F. Liu, J. Liu, and H. Chen (2002). Crust and upper mantle structure beneath western China from P wave travel-time tomography. *J. Geophys. Res*. 107: doi 10.1029/2001JB000402.

Yu, X., Y. Chen, and P. Wang (2003). Three-dimensional P wave velocity structure in Beijing-Tianjin-Tangshan area. *Acta Seismol. Sin.* 25: 1–14.

Zhao, D., A. Hasegawa, and S. Horiuchi (1992). Tomographic imaging of P and S wave velocity structure beneath northeastern Japan. *J. Geophys. Res*. 97: 19,909–19,928.

Zhu, J., J. Cao, X. Cai, Z. Yan, and X. Cao (2002). High resolution surface wave tomography in east Asia and west pacific marginal sea. *Chinese J. Geophys*. 45: 679–698.

Zhu, L., R. Zeng, and F. Liu (1990). 3-D P wave velocity structure under the Beijing network area. *Acta Geophys. Sin*. 33: 267–277 (in Chinese).